Journal of the Serbian Chemical Society
JSCS-info@shd.org.rs • www.shd.org.rs/JSCS

ACCEPTED MANUSCRIPT

Journal of the Serbian Chemical Society
JSCS-info@shd.org.rs • www.shd.org.rs/JSCS
J. Serb. Chem. Soc. **00(0)** 1-15 (2026)
JSCS–13666
Original scientific paper
Published DD MM, 2026

Optimizing fabrication of pharmaceutical capsule shell: a factorial design of corncob-MCC/Carrageenan/starch biofilm

JOKO WALUYO[1]*, MUTIARA R. NURFITRIANINGTYAS[1], RIZKY ARDIANSYAH[1], MUJTAHID KAAVESSINA[1], YUSI PRASETYANINGSIH[2], NOOR FITRAH ABU BAKAR[3], AND IBNU T. PURBA[1]

[1]*Chemical Engineering Department, Universitas Sebelas Maret, 57126, Surakarta, Indonesia,* [2]*Chemical Engineering Department, Politeknik TEDC, 50513, Bandung, Indonesia, and* [3]*Faculty of Chemical Engineering, Universiti Teknologi MARA, 40450, Shah Alam, Selangor, Malaysia.*

(Received 8 December 26025; revised 26 December 2025; accepted 11 May 2024)

Abstract: This study develops biodegradable soft-capsule films using carrageenan, tapioca starch, glycerol, and microcrystalline cellulose (MCC) derived from corncob waste as a halal- and vegetarian-friendly alternative to gelatin. A 2^3 factorial design evaluated the effects of carrageenan (15–25 wt%), MCC (5–15 wt%), and glycerol (10–20 wt%) on tensile strength (TS), elongation (EL), and Young's modulus (YM). The produced biofilms were characterized using mechanical testing, FTIR, XRD, SEM, TGA, disintegration tests, and ANOVA. Mechanical performance varied widely among samples. Among the synthesized biofilms, Sample 2 exhibited the highest tensile strength (6.565 MPa) and Young's modulus (97.029 MPa), while Sample 5 showed the greatest ductility and dissolution time, reaching approximately 20% and 12 minutes, respectively, indicating rapid water-induced matrix breakdown associated with the hygroscopic nature of the polysaccharide-based system. Regression models were highly reliable, with R^2 values of 94.02%, 97.96%, and 96.78% for TS, EL, and YM, respectively. XRD confirmed MCC crystallinity of 62.6%. The TGA results confirm the films' thermal stability and show moisture uptake and char residue consistent with the other analyses. Overall, the carrageenan–starch–MCC-glycerol system offers tunable properties, although further optimization is required for moisture control and purity.

Keywords: biodegradable film; biomass utilization; medicine packaging; sustainable packaging.

INTRODUCTION

Capsule shells play a vital role in oral dosage forms by encapsulating active pharmaceutical ingredients, protecting taste, enhancing swallowability, and

* Corresponding author. E-mail: jokowaluyo@staff.uns.ac.id
https://doi.org/10.2298/JSC251208025W

maintaining stability. Traditionally, soft and hard capsule shells depend heavily on gelatin, a biopolymer derived from partially hydrolyzed animal collagen.[1] Gelatin's favorable dissolution properties and film-forming ability have made it the standard in the pharmaceutical industry.[2] However, the leading global sources of gelatin, namely porcine, contribute 46%, bovine hides 29.4%, and pork and cattle skeletons 23.1% of the total gelatin production, which limits its acceptance among certain groups, including Muslims, vegetarians, and vegans.[3]

In response to these limitations, considerable research has focused on plant- or marine-derived polymers as potential materials for shells. Polysaccharides such as carrageenan (extracted from red seaweed) and plant-derived starches have emerged as promising alternatives. Carrageenan offers gelation, film-forming, and stabilizing functions,[4] while starch contributes to capsule biofilms by forming a continuous, biodegradable polymer network that can be tailored via its amylose/amylopectin ratio, plasticizers, and co-polymers to provide mechanical strength, flexibility, and suitable barrier properties for pharmaceutical use.[5,6] Yet, simple carrageenan–starch systems may suffer from brittleness, limited flexibility, or irregular morphology,[7,8] which suggests the need for additional reinforcing or modifying agents.

One such candidate is microcrystalline cellulose (MCC), a semi-crystalline derivative of cellulose obtained through acid hydrolysis of α-cellulose,[9] characterized by a typical particle diameter of 10–50 μm, a particle length of 100–1000 μm, and crystallinity indices ranging from 60% to 80%.[10] MCC is widely used as a filler, binder, and disintegrant in pharmaceutical tablet formulations, owing to its superior mechanical performance and compressibility.[11] When incorporated into film-forming matrices, MCC can act as a reinforcing particulate, reducing brittleness and improving the flexural and tensile strength of polymer films.[12] Furthermore, corncob, as an abundant agricultural by-product in Indonesia, with approximately 33.5 wt% of annual corn production becoming residue,[13] represents a sustainable source of α-cellulose, reported at around 30 wt%.[14] Among the plasticizers used to increase film flexibility, sorbitol and glycerol are the most commonly used. However, glycerol can enhance elongation at break by more than 25% compared to sorbitol, and it also exhibits a moisture uptake rate that is roughly twice as high.[15]

In this study, a composite biofilm system based on tapioca starch, carrageenan, corncob-MCC and glycerol is proposed as a sustainable alternative for medicine shell capsules. The carrageenan–starch matrix provides the necessary gelation and film-forming behaviour, while MCC and glycerol enhance mechanical strength, flexibility, and durability. Systematically, a two-level factorial design (2^3) is applied to screen the main and interaction effects of carrageenan, MCC, and glycerol on tensile strength, elongation, and Young's modulus. Biofilms prepared under controlled casting conditions will be assessed through ANOVA and

subjected to morphological, chemical, thermal, and disintegration analyses. The development of a mechanically robust, halal-product, and vegetarian-compliant capsule material is expected to contribute meaningfully to advancing sustainable pharmaceutical excipient technology.

EXPERIMENTAL

Materials

The materials employed in this research comprised corncobs as the biomass feedstock, along with sodium hydroxide (NaOH), sodium hypochlorite (NaOCl), and hydrochloric acid (HCl) as chemical reagents. Carrageenan, tapioca starch, and glycerol were utilized as biopolymers, matrices, and plasticizers, respectively. All preparations and experimental procedures were conducted using distilled water to ensure the purity and consistency of the reactions.

Raw material preparation

The collected corncobs were thoroughly washed and subsequently milled to obtain a fine powder, which was later utilized as the feedstock for α-cellulose isolation. To eliminate residual impurities, the powdered material was pretreated with distilled water at 70°C for one hour under constant heating. The preheated sample was then filtered and oven-dried at 60°C for 24 hours.

Isolation of α-cellulose from corncob

Dried corncob powder (20 g) was treated with 600 mL of 0.5 M NaOH solution under ultrasonic agitation at 40 °C for 30 min. Following sonication, the suspension was filtered through a mesh bag and thoroughly rinsed with distilled water until the filtrate achieved a neutral pH. The resulting material was then immersed in 250 mL of 5.25% (v/v) NaOCl solution and allowed to stand for 30 minutes. Subsequently, the mixture was heated at 50°C for 30 minutes, re-filtered, washed, and oven-dried at 60°C for 18 hours to obtain the pretreated corncob sample.

Preparation of microcrystalline cellulose

Microcrystalline cellulose was synthesized through the acid hydrolysis of purified α-cellulose using hydrochloric acid. In this procedure, 50 mL of 3 M HCl was reacted with the α-cellulose at 80 °C for 30 minutes to initiate depolymerization. After the reaction, the resulting MCC was repeatedly rinsed with distilled water until a neutral pH was achieved, ensuring the removal of residual acid. The neutralized material was subsequently filtered and oven-dried at 60 °C for 4 hours, yielding a fine white MCC powder suitable for further processing.

Preparation of soft capsule biofilm

Carrageenan, MCC, and tapioca starch were thoroughly blended and dispersed in 100 mL of distilled water to obtain a uniform mixture. The suspension was subsequently heated to 70–80°C under continuous stirring for approximately five minutes to ensure complete dissolution. Thereafter, glycerol was incorporated into the mixture and stirred for an additional five minutes. The resulting solution was carefully poured into molds and oven-dried at 60°C for 18 hours.

Sample characterization

Analytical techniques included Fourier transform infrared spectroscopy (FTIR, Shimadzu, Japan), X-ray diffraction (XRD, Bruker D8 Advance, USA), scanning electron microscopy (SEM, Quanta 250, Netherlands), and thermogravimetric analysis with differential scanning calorimetry (TGA/DSC, LINSEIS STA PT-1600, Germany). FTIR was used to identify

functional groups in corncob, MCC, and capsule films, while XRD evaluated crystalline structures. SEM examined the surface morphology, and TGA assessed moisture-related mass loss, hygroscopic behavior, and thermal stability. Mechanical properties were measured using a universal testing machine (HZ-1007A, Lyxyan, China) in accordance with ASTM D683-14.

Analytical methods

The analysis focused on 2^3 factorial design that was carried out by Design Expert v25.0 the percentage composition of carrageenan (15, 20, and 25 wt%), MCC (5, 10, and 15 wt%), glycerol (10, 15, and 20 wt%), and tapioca starch (by difference) in response to tensile strength (TS), elongation (EL), and Young's modulus (YM) of the capsule shell biofilm. According to Equations (1–3), tensile strength was determined as the tensile force divided by the cross-sectional area, elongation as the ratio of length increase to initial length, and Young's modulus as the ratio of stress to strain. ANOVA was performed to determine the optimal values for each film characteristic. The composition of each sample is tabulated in Table I.

$$TS(\sigma) = \frac{F}{A} \quad (1)$$

$$EL(\varepsilon) = \frac{\Delta L}{L} \times 100\% \quad (2)$$

$$YM(\gamma) = \frac{\sigma(stress)}{\varepsilon(strain)} ss \quad (3)$$

TABLE I Sample composition

Run	Carrageenan (%)	MCC (%)	Glycerol (%)	Starch (%)
1	25	5	20	50
2	15	5	10	70
3	25	5	10	60
4	15	15	20	50
5	25	15	10	50
6	20	10	15	55
7	15	5	20	60
8	25	15	20	40
9	20	10	15	55
10	15	15	10	60

RESULTS AND DISCUSSION

Based on laboratory observations, 10 film samples were prepared according to Table I and shown in Fig. S1 to serve as candidate materials for drug capsule shells. The samples were subsequently evaluated to confirm the successful synthesis of MCC, determine the optimal film formulation suitable for capsule fabrication, and assess their initial physical characteristics prior to further analyses, including FTIR, SEM, TGA, and disintegration testing in accordance with the Indonesian Pharmacopoeia,[16] and statistical evaluation using ANOVA.

Mechanical test

The mechanical test results for each sample are shown in Table II. Analysis of variance (ANOVA) revealed that the interaction between carrageenan and glycerol significantly influences tensile strength. Elongation is determined by the

individual effects of carrageenan and MCC, as well as their combined interaction. Meanwhile, Young's modulus is governed by the synergistic interactions of carrageenan/glycerol/MCC/starch. The statistical model derived from the ANOVA results is presented in Tables SI-SIII, and the fit statistic for each response is tabulated in Table SIV.

TABLE II Mechanical test results (dual repetition)

Sample	TS (MPa)		EL (%)		YM (MPa)	
	1	2	1	2	1	2
1	3.374	3.728	10.324	9.198	32.681	40.531
2	5.082	6.565	5.753	6.766	88.337	97.029
3	6.015	5.080	11.623	11.661	51.751	43.564
4	2.073	2.209	8.569	7.720	24.192	28.614
5	4.848	4.682	20.192	18.774	24.010	24.939
6	5.39	3.842	10.09	11.272	53.419	34.084
7	2.638	3.035	8.758	10.260	30.121	29.581
8	0.981	1.623	8.803	7.565	11.144	21.454
9	5.626	4.459	10.626	10.486	52.946	42.523
10	4.794	4.900	7.403	6.179	64.758	79.301

Based on Table II, the mechanical test results show clear variations in strength, ductility, and stiffness across the 10 samples. Sample 2 demonstrates the highest overall performance, with TS reaching 6.565 MPa and YM up to 97.029 MPa, indicating a strong and stiff material; however, its low elongation at break (~6%) suggests limited flexibility and more brittle behavior. At the opposite end, Sample 8 shows the lowest TS (0.981–1.623 MPa) and YM (11.144–21.454 MPa), indicating a weak, highly compliant material. Sample 5 achieves the greatest elongation at break (18–20%), offering superior ductility despite only moderate strength. These differences illustrate the trade-offs among strength, stiffness, and flexibility, with some formulations favoring rigidity (Sample 2), others favoring deformability (Sample 5), and some exhibiting the lowest structural performance (Sample 8). Biofilms for soft capsule applications intended to replace porcine gelatin should exhibit tensile strength within 2.4–63.25 MPa and elongation of 4.4–90.55%.[17] Based on these criteria, Samples 4 and 8 do not meet the required specifications because their tensile strength values fall below the acceptable range.

The statistical summary provides a solid basis for evaluating the validity of the regression models (Table SIV). The coefficient of variation (C.V.), defined as the ratio of standard deviation to the mean, is used to assess data dispersion, precision, and reproducibility. In empirical studies, a C.V. <10% is considered indicative of high precision[18]. In this study, C.V. values for TS (18.91%) and YM (15.52%) reflect moderate variability, suggesting that subtle differences between

treatments might approach the limit; by contrast, EL shows a C.V. of 7.68%, indicating relatively high precision under the experimental conditions.

The regression models for TS, EL, and YM demonstrate strong explanatory and predictive performance. EL and YM show high adjusted R^2 values (0.9552 and 0.9149), capturing over 90% of response variability, while TS has an adjusted R^2 of 0.7543, explaining about 75%. Adjusted R^2 is preferred because it accounts for multiple predictors and reduces overfitting risk. The predicted R^2 values (0.9112 for EL, 0.8748 for YM, and 0.6776 for TS) fall within 0.20 of their respective adjusted R^2 values, meeting established reliability criteria and confirming good predictive capability within the design space.[19]

Furthermore, the adequate precision values (signal-to-noise ratios) for all three models exceed the minimum threshold of 4, indicating acceptable model discrimination and response-surface reliability.[20] The high signal-to-noise ratios confirm that the coded regression models reliably capture the response trends and are suitable for probing factor interactions and guiding formulation optimization. Overall, the models (Equations 4–6) provide a robust representation of how carrageenan (A), MCC (B), and glycerol (C) influence TS, EL, and YM. The predicted vs actual plot is illustrated in Fig. S2-S4 for each response.

$$TS = 4.05 - 0.06A - 0.59B - 1.39C - 0.17AB + 0.03AC - 0.15BC - 0.22ABC \quad (4)$$

$$EL = 10.10 + 2.30A + 0.68B - 1.07C + 0.89AB - 2.22AC - 1.41BC - 0.94ABC \quad (5)$$

$$YM = 43.25 - 11.99A - 8.45B - 15.96C - 2.42AB + 11.15AC + 2.51BC - 1.79ABC \quad (6)$$

The 3D-surface and contour plots show how carrageenan (A), MCC (B), and glycerol (C) affect TS, EL, and YM, and which combinations maximize each response. Fig. 1 shows their effect on EL response. The AC interaction critically governs the balance between stiffness and ductility in the films. At low to moderate carrageenan contents, increasing glycerol significantly enhances elongation at break by increasing chain mobility and weakening intermolecular hydrogen bonding within the polysaccharide matrix. However, at higher carrageenan levels, the reinforcing effect of carrageenan increasingly restricts chain motion, reducing glycerol's plasticization efficiency and leading to greater stiffness. This antagonistic behavior explains the strong AC interaction observed for Young's modulus, where stiffness is controlled by the competition between matrix reinforcement and plasticizer-induced flexibility. For TS (Fig. S5), the BC interaction further defines the strength–ductility trade-off, i.e., MCC enhances tensile strength through rigid reinforcement and efficient stress transfer at low glycerol levels, whereas increasing glycerol progressively disrupts filler–matrix interactions, reducing tensile strength. While the B loading is higher, it suppresses elongation at break. Excessive glycerol addition results in visibly wet, tacky films, indicating matrix oversaturation that compromises mechanical integrity and underscores the need for a controlled plasticizer content to maintain an optimal

balance among strength, flexibility, and dimensional stability. The highest YM was observed when A, B, and C were kept low (Fig. S6).

Disintegration test

As reported in a previous study, the mean disintegration time (DT) in 0.1 N HCl was approximately 18 minutes.[17] The experimental outcomes, summarized in Table III, reveal distinct variations among the tested samples. Notably, Samples 3 and 5 demonstrated the most hygroscopic (< 20 min), achieving complete disintegration within 16 and 12 minutes, respectively, which is markedly faster than the average and significantly lower than the times observed for other formulations, several of which exceeded 30 minutes. According to the Indonesian Pharmacopoeia,[16] Immediate-release tablets must disintegrate within 30 min, while antifungal and anticholinergic products require <20 and <15 min, respectively. In this context, Sample 5 exhibits enhanced disintegration under acidic conditions, Sample 3 closely meets antifungal specifications, and the slower-disintegrating Samples 7 and 10 are more consistent with delayed- or extended-disintegration formulations. The disintegration behavior of the films is governed by the hygroscopic polysaccharide–glycerol matrix, which facilitates rapid water uptake upon immersion. Absorbed water disrupts intermolecular hydrogen bonding, induces matrix swelling, and leads to swelling-induced structural breakdown of the film.[21] Variations in disintegration time among formulations reflect differences in glycerol content and network rigidity, consistent with the observed mechanical and thermal properties. Therefore, Sample 5 was selected for further characterization as it exhibited the fastest disintegration while maintaining the mechanical performance, making it the most representative formulation.

TABLE III Disintegration test results in 0.1 N HCl solution

Sample	1	2	3	5	7	9	10
DT (Min)	> 30 min	> 30 min	16 min	12 min	26 min	> 30 min	21 min

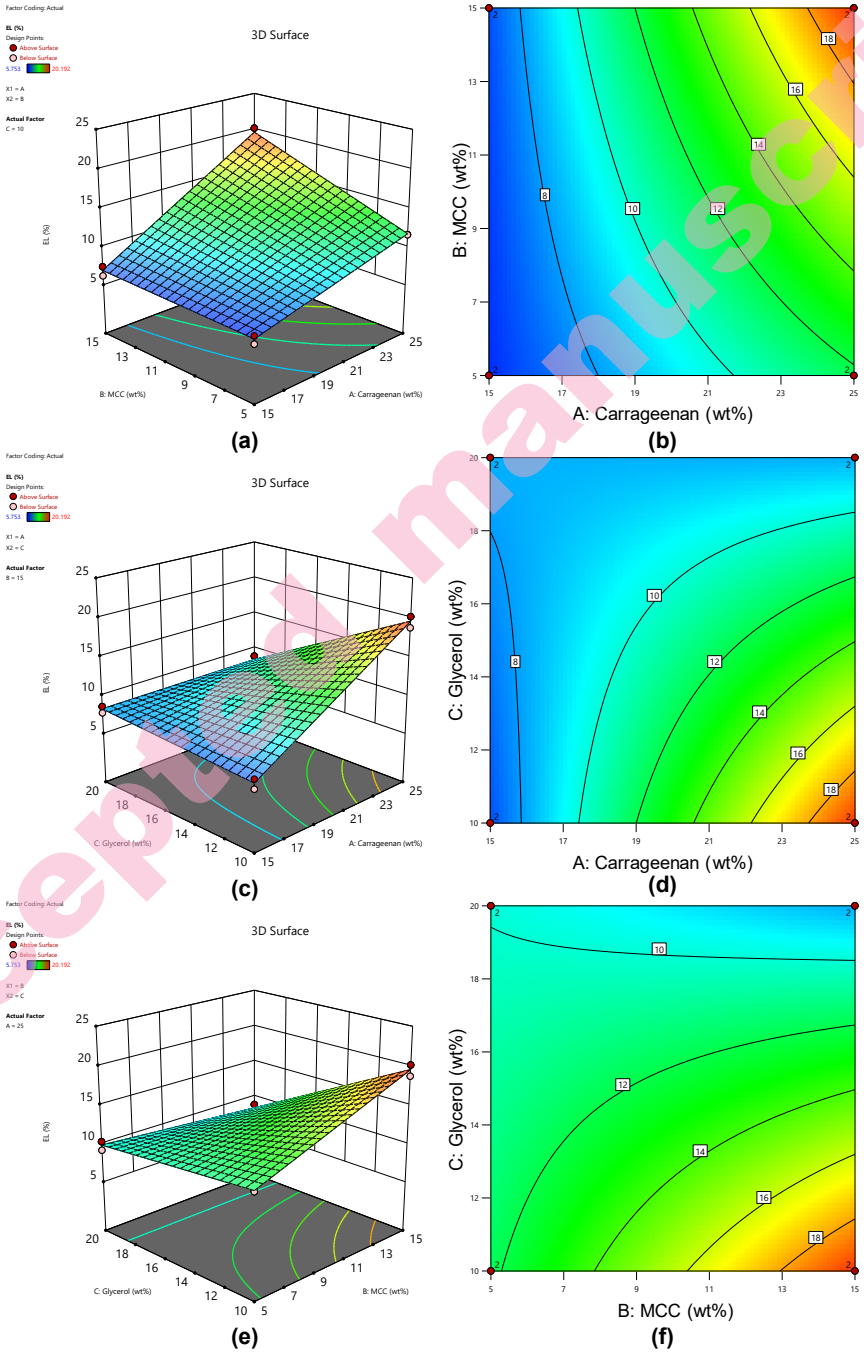

Fig. 1 Surface plot and contour plot of factor influenced on EL: (a,b) carrageenan and MCC, (c,d) carrageenan and glycerol, (e,f) MCC and glycerol

Scanning electron microscope

The SEM observations of the MCC revealed that, under lower magnifications (100× and 250×), the particles exhibited a generally homogeneous distribution. However, occasional larger fragments were still discernible, likely a consequence of incomplete removal during the filtration stage. With increasing magnification (500× and 1000×), the surface morphology displayed distinct microstructural features, such as pores, fissures, and inter-aggregate voids, indicating the presence of interfibrillar regions that may enhance the material's capacity for adsorption and controlled release of active compounds. Based on Fig. 2a and 2b, the MCC used was <200 µm, which aligns with the standard dimensional range for MCC model PHs 101, 102, 103, 112, 113, 200, 301, and 302 (50–180 µm).[22] The isolated sample demonstrated conformity within acceptable limits, affirming the consistency and particle size.

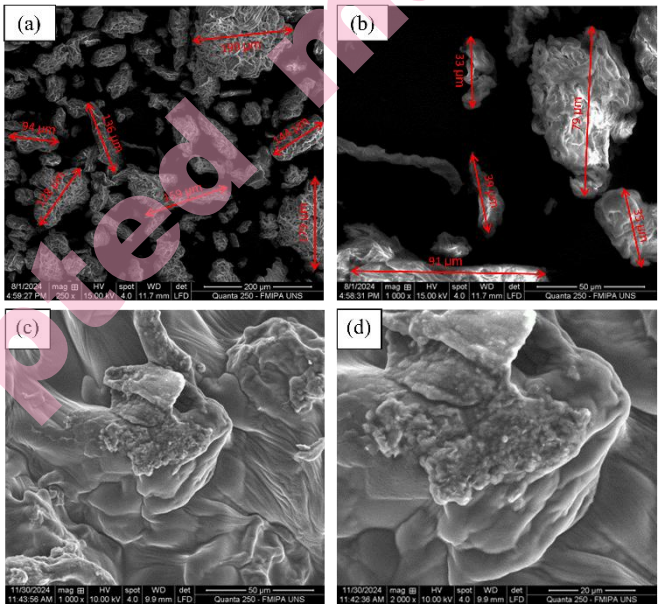

Fig. 2 SEM of MCC: (a) 250× and (b) 1000× magnifications; and biofilm: (c) 1000× and (d) 2000× magnifications.

The SEM micrographs of the biofilm exhibited a distinctly layered morphology at 1000× and 2000× magnification (Fig. 2c and 2d). The surface evolved from heterogeneous aggregated clusters to partially disentangled fibrous structures, ultimately revealing well-defined layered networks that indicate the coexistence of amorphous domains and successful incorporation of microcrystalline cellulose within the biofilm matrix.

Fourier transform infrared analysis

According to Fig. 3a, the FTIR spectra of corncob, MCC, and the capsule biofilm show distinct compositional differences despite overall similarity. All samples display broad O–H stretching at 3500–3200 cm^{-1}, characteristic of MCC showing the sharpest band, which means it has a rich O–H bond.[23,24] Peak 3000–2800 cm^{-1} C–H stretching region appears clearly in corncob and MCC, reflecting cellulose and hemicellulose structures [25,26]. In contrast, the biofilm exhibits a pronounced 1750–1600 cm^{-1} carbonyl band linked to C=O groups from glycerol, starch, and carrageenan.[27] The corncob spectrum shows stronger lignin-associated C=C vibrations at 1600–1500 cm^{-1}, [24]whereas this band is reduced in MCC after delignification.[24] Signals near 1250 cm^{-1} confirm C–O stretching from cellulose and hemicellulose, indicating successful cellulose isolation, while the 1000–1100 cm^{-1} band characteristic of carrageenan highlights C–O–C glycosidic linkages.[28] Overall, FTIR spectroscopy successfully identified functional groups associated with cellulose-based materials and polymer components in the samples. The spectra show absorption bands corresponding to O–H, C–H, and C–O functional groups, indicating the presence of cellulose-related structures and the incorporation of carrageenan, glycerol, and starch in the film matrix. No new absorption bands were observed, suggesting that the film formation is governed by physical interactions rather than chemical modification.

X-Ray diffraction

X-ray diffraction analysis reveals that the MCC isolated from corncob exhibits sharp, well-defined peaks at 2θ = 15.5°, 22.2°, and 34.4°, corresponding to a crystallinity index of 62.6% (Fig. 3b). In contrast, the untreated corncob exhibits broader, less intense peaks, indicating a more amorphous structure and a lower crystallinity of 49.8%. In contrast, the composite Sample 5 exhibits very diffuse diffraction patterns and markedly diminished peak intensity, indicating a substantial disruption of ordered crystalline domains. This loss of long-range order is likely caused by the incorporation of starch and carrageenan, which interfere with the tight packing of cellulose chains and increase free volume in the matrix. Additionally, the incorporation of glycerol into the starch-based matrix is expected to interfere with intermolecular hydrogen bonding interactions.[29] Although no pronounced shift or intensity change is observed in the O–H stretching region (3500–3200 cm^{-1}) in Fig. 3a, a slight broadening and subtle variation in band shape can be discerned. This behavior suggests the formation of new hydrogen bonding interactions between glycerol and polysaccharide chains, which partially replace the native polymer–polymer interactions rather than significantly altering the overall hydroxyl vibrational profile. In response, this action suppresses crystalline domain formation and leads to reduced crystallinity as observed from the decreased XRD diffraction intensity (Fig. 3b), resulting in a more flexible and amorphous film structure. From a functional perspective, the marked reduction in

crystallinity in Sample 5 may confer several advantages for pharmaceutical biofilm or capsule applications. Amorphous polymer systems typically offer greater flexibility and better resistance to stress fracture.[30] However, because amorphous domains generally have higher molecular mobility and a greater tendency to recrystallize over time, it will be essential to assess the physical stability of Sample 5 under storage, including its potential for aging or recrystallization, to ensure long-term performance. Similar phenomena (loss of crystallinity after blending with plasticizers and biopolymers) have been reported in other polysaccharide/glycerol films.[31]

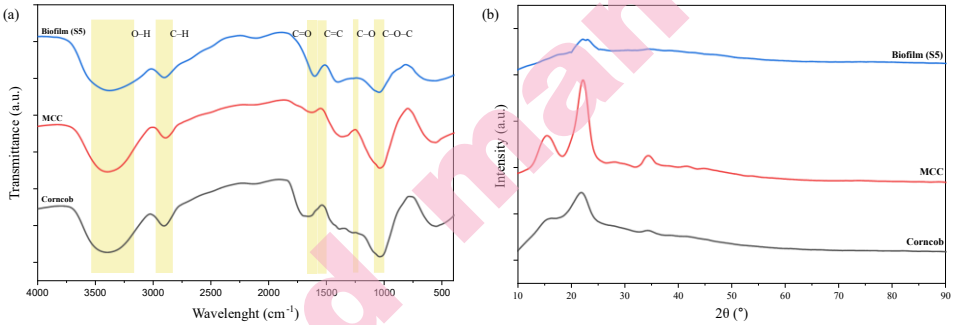

Fig. 3 Spectra analysis of corncobs, capsule biofilms, and MCC: a) FTIR and b) XRD.

Thermogravimetric analysis

For polysaccharide-based capsule materials, low-temperature mass loss is particularly relevant, as it reflects absorbed and bound water that directly influences storage stability and disintegration performance.[32] While the primary thermal degradation occurs above 250 °C, the early-stage mass loss at lower temperatures reflects the film's hygroscopic behavior, which plays a more critical role in determining its storage stability and functional performance in pharmaceutical use.[33] According to Fig.4, both TGA (T_{max}) and DSC results confirm a high cellulose fraction, consistent with the characteristic thermal decomposition of cellulose occurring between 300 and 350 °C: MCC exhibited the highest T_{max}, while S5 showed a slightly lower T_{max} and broader thermal transitions, consistent with reduced crystallinity.

However, the primary limitation for pharmaceutical use is not thermal stability but hygroscopicity, which poses risks for moisture-sensitive drugs. To overcome this issue, partial replacement of glycerol with less hygroscopic plasticizers, e.g., tributyl citrate, and mild crosslinking to reduce free hydroxyl groups and thereby reduce moisture uptake. Additionally, the relatively high char residue (~16% at 700 °C) warrants attention. Similar trends have been reported for MCC derived from corncob and for carrageenan-based capsules, which can yield

11.8–17.7% char, indicating the persistence of non-volatile structural components or trace impurities even after purification.[34]

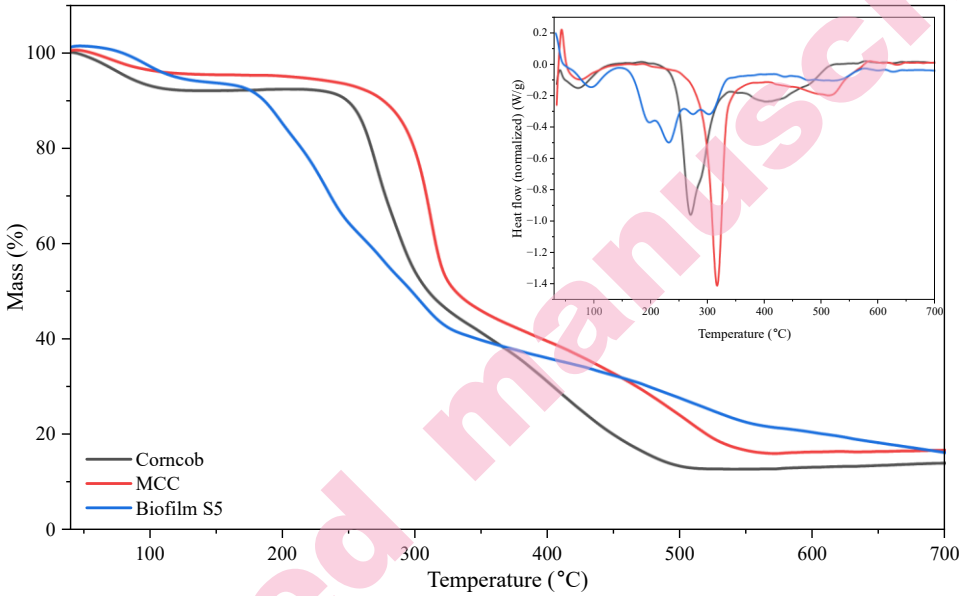

Fig. 4 TGA and DSC spectra.

CONCLUSION

This study quantitatively elucidates the individual and interaction effects of carrageenan, MCC, and glycerol on the mechanical performance of bio-based capsule films using a 2^3 factorial design. Statistical analysis shows that glycerol is the dominant factor controlling tensile strength (p-value <0.01%), while MCC enhances stiffness and load-bearing capacity. Elongation at break is governed by both main and interaction effects (p-value < 5%), demonstrating the coupled roles of polymer matrix composition and plasticization in regulating film ductility. This study observed TS ranged from 1.0 to 6.6 MPa, EL from 5.8 to 20.2%, and YM from 11.1 to 97 MPa. TS is maximized by increasing MCC content while minimizing glycerol, elongation is enhanced by higher carrageenan and glycerol contents with reduced MCC loading, and Young's modulus is maximized when carrageenan, MCC, and glycerol are all kept at low levels. Despite moderate experimental variability, the models exhibited strong predictive capability. The disintegration time results in accordance with the Indonesian Pharmacopoeia, demonstrating that the hygroscopic polysaccharide–glycerol matrix facilitates water uptake and swelling-induced structural breakdown. Combined XRD, FTIR, and TGA/DSC demonstrate that glycerol-induced disruption of hydrogen bonding reduces film crystallinity and thermal stability, increasing amorphous character

and hygroscopicity. These findings provide practical guidance for formulating plant-based pharmaceutical capsule films by balancing mechanical performance, disintegration behavior, and moisture stability.

SUPPLEMENTARY MATERIAL

Additional data are available electronically at the pages of journal website: https://www.shd-pub.org.rs/index.php/JSCS/article/view/13666, or from the corresponding author on request.

Acknowledgements: The authors extend their sincere appreciation for the financial support provided through the Research Group Grant from Universitas Sebelas Maret under Award No. 370/UN27.22/PT.01.03/2025, which made this work possible.

И З В О Д

ОПТИМИЗАЦИЈА ИЗРАДЕ ОМОТАЧА ФАРМАЦЕУТСКЕ КАПСУЛЕ: ФАКТОРИЈАЛНИ ДИЗАЈН БИОФИЛМА КУКУРУЗНА МИКРОЦЕЛУЛОЗА/КАРАГЕНАН/СКРОБ

JOKO WALUYO[1*], MUTIARA R. NURFITRIANINGTYAS[1], RIZKY ARDIANSYAH[1], MUJTAHID KAAVESSINA[1], YUSI PRASETYANINGSIH[2], NOOR FITRAH ABU BAKAR[3], IBNU T. PURBA[1]

[1]Chemical Engineering Department, Universitas Sebelas Maret, 57126, Surakarta, Indonesia, [2]Chemical Engineering Department, Politeknik TEDC, 50513, Bandung, Indonesia, and [3]Faculty of Chemical Engineering, Universiti Teknologi MARA, 40450, Shah Alam, Selangor, Malaysia.

У овој студији су развијани биоразградиви филмови меких капсула користећи карагенан, тапиока скроб, глицерол и микрокристалну целулозу (MCC), која је добијена из отпада кукурузног клипа као халал и вегетаријанска алтернатива желатину. 2^3 факторијални дизајн је коришћен за процену утицаја удела карагенана (15–25 мас. %), MCC (5–15 мас.%) и глицерола (10–20 мас.%) на затезну чврстоћу (TS), издужење (EL) и Јангов модул еластичности (YM). Произведени биофилмови су окарактерисани применом механичких испитивања, FTIR, XRD, SEM, TGA, тестова дезинтеграције и ANOVA. Механичке перформансе су се значајно разликовале међу узорцима. Узорак 2 је показао највећу затезну чврстоћу (6,565 MPa) и Јангов модул еластичности (97,029 MPa), док је узорак 5 показао највећу дуктилност и време растварања, достижући приближно 20% и 12 минута, редом, што указује на брзу разградњу матрице под дејством воде услед хигроскопне природе полисахаридог система. Регресиони модели су били веома поуздани, са R^2 вредностима од 94,02%, 97,96% и 96,78% за TS, EL и YM, редом. Кристалиничност MCC, одређена XRD анализом, износила је 62,6%. Резултати TGA су потврдили термичку стабилност филмова и показали апсорпцију влаге и заостали угљеник у складу са осталим анализама. Генерално, својства система карагенан-скроб-MCC-глицерол се могу лако подешавати, при чему је потребна даља оптимизација за контролу влаге и чистоће.

(Примљено 8. децембра 2025; ревидирано 26. децембра 2025; прихваћено 11. маја 2026.)

REFERENCES

1. A. Rohman, A. Windarsih, I. Musfiroh, V. Maritha, Wirnawati, D. Lestari, D. Hamidi, Y. Susanto, N. K. A. Bakar, *J. Appl. Pharm. Sci.* **15** (2025) 026–034 (https://doi.org/10.7324/japs.2025.203667)
2. X. Xu, Y. Xi, Y. Weng, *RSC Adv.* **15** (2025) 30605–30621 (https://doi.org/10.1039/d5ra03325j)
3. J. Alipal, N. A. S. Mohd Pu'ad, T. C. Lee, N. H. M. Nayan, N. Sahari, H. Basri, M. I. Idris, H. Z. Abdullah, *Mater. Today Proc.* **42** (2021) 240–250 (https://doi.org/10.1016/j.matpr.2020.12.922)
4. T. Udo, G. Mummaleti, A. Mohan, R. K. Singh, F. Kong, *Food Res. Int.* **173** (2023) 113369 (https://doi.org/10.1016/j.foodres.2023.113369)
5. G. P. Singh, S. P. Bangar, T. Yang, M. Trif, V. Kumar, D. Kumar, *Polymers (Basel)* **14** (2022) 1987 (https://doi.org/10.3390/polym14101987)
6. I. Kong, P. Degraeve, L. P. Pui, *Foods* **11** (2022) 555 (https://doi.org/10.3390/foods11040555)
7. E. S. Madivoli, J. Kisato, P. K. Kimani, K. Kamau, *Food Sci. Nutr.* **13** (2025) e4664 (https://doi.org/10.1002/fsn3.4664)
8. F. Jabeen, N. Zil-E-Aimen, R. Ahmad, S. Mir, N. S. Awwad, H. A. Ibrahium, *RSC Adv.* **15** (2025) 22035–22062 (https://doi.org/10.1039/d5ra03296b)
9. P. M. Raja, I. U. P. Rangkuti, M. Hendra Ginting, Giyanto, W. F. Siregar, *IOP Conf. Ser. Earth Environ. Sci.* **819** (2021) 012002 (http://doi.org/10.1088/1755-1315/819/1/012002)
10. P. T. Arnandan, W. N. Nadyaini Wan Omar, Z. H. Hassan, M. S. Abd Muhaimin, D. A. Jihat Ahmad, M. M. Michele Raissa, A. Shamjuddin, K. L. Chang, N. A. S. Amin, *Biomass Bioenergy* **199** (2025) 107902 (https://doi.org/10.1016/j.biombioe.2025.107902)
11. N. E. Alamdari, B. Aksoy, R. J. Babu, Z. Jiang, *Int. J. Biol. Macromol.* **270** (2024) 132298 (https://doi.org/10.1016/j.ijbiomac.2024.132298)
12. E. Gorgun, A. Ali, M. S. Islam, *ACS Omega* **9** (2024) 11523–11533 (https://doi.org/10.1021/acsomega.3c08448)
13. J. Campos Silva, A. Jayane Nunes Siqueira, H. Bezerra Maia, R. Rachide Nunes, *Bioresour. Technol. Rep.* **15** (2021) 100730 (https://doi.org/10.1016/j.biteb.2021.100730)
14. D. Sartika, A. P. Firmansyah, I. Junais, I. W. Arnata, F. Fahma, A. Firmanda, *Int. J. Biol. Macromol.* **240** (2023) 124327 (https://doi.org/10.1016/j.ijbiomac.2023.124327)
15. K. Zhou, Y. Yang, B. Zheng, Q. Yu, Y. Huang, N. Zhang, S. M. Rama, X. Zhang, J. Ye, M. Xiao, *Polymers (Basel)* **15** (2023) 2247 (https://doi.org/10.3390/polym15102247)
16. Kemenkes, *Farmakope Indonesia Edisi VI*, Jakarta, 2020 (https://farmalkes.kemkes.go.id/2020/11/farmakope-indonesia-edisi-vi/).
17. A. Naharros-Molinero, M. Á. Caballo-González, F. J. de la Mata, S. García-Gallego, *Adv. Healthc. Mater.* **13** (2024) 2302250 (https://doi.org/10.1002/adhm.202302250)
18. A. E. Mariño-Gámez, M. E. Juarez-Huitron, J. A. Aguilar-Martínez, L. Felipe-Verdeja, L. V. García-Quiñonez, C. Gómez-Rodríguez, *J. Comp. Sci.* **9** (2025) 555 (https://doi.org/10.3390/jcs9100555)

19. E. Gholamzadeh, A. Shokri, A. Ghaemi, B. Heydari, *Sci. Rep.* **15** (2025) 38763- (https://doi.org/10.1038/s41598-025-22629-4)
20. N. R. Draper, H. Smith, *Applied regression analysis*, 3rd ed., John Wiley & Sons, Inc., New York, 1998 (https://doi.org/10.1002/9781118625590)
21. F. N. Ainin, M. D. Azaman, L. M. Ferreira, C. A. C. P. Coelho, M. S. Abdul Majid, M. J. M. Ridzuan, *Polym. Compos.* **47** (2025) 1895–1911 (https://doi.org/10.1002/pc.70264)
22. S. S. Z. Hindi, *Nanosci. Nanotech. Res.* **4** (2017) 17–24 (https://doi.org/10.12691/nnr-4-1-3)
23. Y. Wang, G. Huang, *Sci. Rep.* **15** (2025) 6331- (https://doi.org/10.1038/s41598-025-90697-7)
24. J. Waluyo, I. T. Purba, K. Q. Sani, N. Sayekti, S. S. Ramadhani, S. H. Pranolo, Margono, M. Kaavessina, *J. Plast. Film Sheet.* **40** (2024) 259–282 (https://doi.org/10.1177/87560879231226442)
25. A. Kassem, L. Abbas, O. Coutinho, S. Opara, H. Najaf, D. Kasperek, K. Pokhrel, X. Li, S. Tiquia-Arashiro, *Front. Microbiol.* **14** (2023) 1304081 (https://doi.org/10.3389/fmicb.2023.1304081)
26. I. T. Purba, K. Q. Sani, N. Sayekti, S. S. Ramadhani, J. Waluyo, S. H. Pranolo, M. Kaavessina, *IOP Conf. Ser. Earth Environ. Sci.* **1217** (2023) 012037 (https://doi.org/10.1088/1755-1315/1217/1/012037)
27. A. B. D. Nandiyanto, R. Ragadhita, M. Fiandini, *Indonesian J. Sci. Technol.* **8** (2023) 113–126 (https://doi.org/10.17509/ijost.v8i1.53297)
28. S. Pasieczna-Patkowska, M. Cichy, J. Flieger, *Molecules* **30** (2025) 684 (https://doi.org/10.3390/molecules30030684)
29. J. Tarique, S. M. Sapuan, A. Khalina, *Sci. Rep.* **11** (2021) 13900 (https://doi.org/10.1038/s41598-021-93094-y)
30. Poly Fluoro, *Poly Fluoro Ltd* (2024) (https://polyfluoroltd.com/blog/crystalline-vs-amorphous-polymers-structural-overview/). Published November 27, 2024. Accessed November 16, 2025.
31. D. Domene-López, J. C. García-Quesada, I. Martin-Gullon, M. G. Montalbán, *Polymers (Basel)* **11** (2019) 1084 (https://doi.org/10.3390/polym11071084)
32. A. Patel, C. Jin, B. Handzo, R. Kalyanaraman, *J. Pharm. Biomed. Anal.* **229** (2023) 115381 (https://doi.org/10.1016/j.jpba.2023.115381)
33. L. You, J. Bour, Y. Fleming, B. Marcolini, P. Fischer, C. Soukoulis, *Food Hydrocoll.* **170** (2026) 111663 (https://doi.org/10.1016/j.foodhyd.2025.111663)
34. M. Al Rizqi Dharma Fauzi, P. Pudjiastuti, E. Hendradi, R. Teguh Widodo, *J. Saudi Chem. Soc.* **27** (2023) 101672 (https://doi.org/10.1016/j.jscs.2023.101672).